

An adaptive homotopy method for computing bifurcations of nonlinear parametric systems

Wenrui Hao *

Chunyue Zheng †

Abstract

In this paper, we present an adaptive step-size homotopy tracking method for computing bifurcation points of nonlinear systems. There are four components in this new method: 1) an adaptive tracking technique is developed near bifurcation points; 2) an inflation technique is backed up when the adaptive tracking fails; 3) Puiseux series interpolation is used to compute bifurcation points; and 4) the tangent cone structure of the bifurcation point is approximated numerically to compute solutions on different branches. Various numerical examples of nonlinear systems are given to illustrate the efficiency of this new approach. This new adaptive homotopy tracking method is also applied to a system of nonlinear PDEs and shows robustness and efficiency for large-scale nonlinear discretized systems.

Keywords: adaptive homotopy tracking, bifurcation computation, nonlinear systems.

1 Introduction

Many mathematical models of natural phenomena, e.g., biology [22], physics [25, 26] and materials science [28], involve systems of nonlinear equations [14, 19, 20, 22]. From a mathematical point of view, studies of these nonlinear equations can be formulated numerically and theoretically to focus on solution structures such as bifurcations [40, 41]. Theories and numerical methods have contributed to a better

*Department of Mathematics, Pennsylvania State University, University Park, PA 16802, USA.
Email: wxh64@psu.edu

†Department of Mathematics, Pennsylvania State University, University Park, PA 16802, USA.
Email: cmz5199@psu.edu

understanding of these solution structures, in which the bifurcation between solutions and parameters is the central question [17, 43]. Although theory helps us to understand the solution structures in many cases [15, 16], the in-depth and more quantitative study of these problems often requires large-scale simulations to numerically compute bifurcations. A bifurcation occurs in a nonlinear parametric system when the parameter change causes the solution structure to change. There are many types of bifurcations, such as saddle-node bifurcation, transcritical bifurcation, pitchfork bifurcation, and Hopf bifurcation with different theoretical classifications [30]. However computing these different bifurcation points numerically brings the same numerical challenge. In specific, this corresponds to the real part of an eigenvalue of the Jacobian passing through zero and causes numerical challenges for Newton's and Newton-like methods [11, 50, 49]. Therefore, efficient numerical methods for computing bifurcations of large-scale systems are keys to understanding these systems.

The homotopy continuation method [35, 36, 37, 38] has been successfully used to compute bifurcations and structural stabilities for studying parametric problems. Recently, several numerical methods based on homotopy continuation methods have been developed for computing bifurcation points of nonlinear PDEs [21, 22]. These numerical methods have also been applied to hyperbolic conservation laws [23], physical systems [25, 26] and some more complex free boundary problems arising from biology [19, 20]. However, the computational cost becomes more expensive and the efficiency becomes low when they are applied to large-scale systems. Therefore, an efficient homotopy continuation method for computing bifurcation is needed to deeply study the large-scale nonlinear systems. In this paper, we will present an efficient adaptive homotopy tracking method that integrates numerical methods from numerical algebraic geometry and scientific computing so that we can apply this efficient method to compute bifurcation points of large-scale nonlinear systems such as discretized systems arising from nonlinear PDEs.

2 Homotopy Continuation Method

In this section, we will first give an overview of the homotopy continuation method. Generally speaking, a nonlinear parametric system is written as $\mathbf{F} : \mathbb{R}^n \times \mathbb{R} \rightarrow \mathbb{R}^n$,

$$\mathbf{F}(\mathbf{u}, p) = \mathbf{0}, \quad (1)$$

where p is a parameter and \mathbf{u} is the variable vector [2, 39] that depends on the parameter p , namely, $\mathbf{u} = \mathbf{u}(p)$. We want to start with solutions that are easy to find (e.g., radially symmetric solutions in nonlinear PDEs [21]) in order to compute

the bifurcation points where the other more interesting solutions come from (e.g., non-radial solution [21]). For this parametric system, the standard homotopy continuation method [10, 46] uses a predictor/corrector method to track the solution \mathbf{u} as the parameter p varies. Basic prediction and correction are both accomplished by considering a local model via its Taylor expansion:

$$\mathbf{F}(\mathbf{u} + \Delta\mathbf{u}, p + \Delta p) = \mathbf{F}(\mathbf{u}, p) + \mathbf{F}_{\mathbf{u}}(\mathbf{u}, p)\Delta\mathbf{u} + \mathbf{F}_p(\mathbf{u}, p)\Delta p + \text{Higher-Order Terms},$$

where $\mathbf{F}_{\mathbf{u}} = \partial\mathbf{F}/\partial\mathbf{u}$ is the $n \times n$ Jacobian matrix and $\mathbf{F}_p = \partial\mathbf{F}/\partial p$ has size $n \times 1$.

2.1 Predictor-Corrector Method

The Predictor-Corrector method consists of two parts: the first one is the predictor step which gives a prediction of $\Delta\mathbf{u}$ for any given Δp based on numerical methods for solving ordinary differential equation such as Euler method, the secant predictor method, and etc (see [1] for more details); the second one is the corrector method which refines the predicted solution based on numerical methods for solving nonlinear systems such as Newton's method, conjugate gradient methods and etc (see [1] for more details). In this section, we will use the Euler predictor and the Newton corrector to illustrate the idea of the predictor-corrector procedure. Other predictor-corrector method can be found in [1]. Given a solution (\mathbf{u}_0, p_0) on the path, that is, $\mathbf{F}(\mathbf{u}_0, p_0) = 0$, we plan to compute a solution at $p_1 = p_0 + \Delta p$ by setting $\mathbf{F}(\mathbf{u}_0 + \Delta\mathbf{u}, p_0 + \Delta p) = 0$. First we make an Euler predictor step, solving the first-order terms $\mathbf{F}_{\mathbf{u}}(\mathbf{u}_0, p_0)\Delta\mathbf{u} = -\mathbf{F}_p(\mathbf{u}_0, p_0)\Delta p$, and then letting $\tilde{\mathbf{u}}_1 = \mathbf{u}_0 + \Delta\mathbf{u}$. On the other hand, when $\|\mathbf{F}(\tilde{\mathbf{u}}_1, p_1)\|$ is not sufficiently small, one may fix p_1 to be constant by setting $\Delta p = 0$ and solving the following equation by using the Newton corrector: $\mathbf{F}_{\mathbf{u}}(\tilde{\mathbf{u}}_1, p_1)\Delta\mathbf{u} = -\mathbf{F}(\tilde{\mathbf{u}}_1, p_1)$. Repeat this corrector step until $\|\mathbf{F}(\tilde{\mathbf{u}}_1, p_1)\|$ is smaller than the chosen tolerance criterion, then we can get $\mathbf{u}_1 = \tilde{\mathbf{u}}_1 + \Delta\mathbf{u}$ and (\mathbf{u}_1, p_1) is on the path (see an illustration in Fig. 1).

2.2 The Step-Size Control

The main concern of a numerical path-tracking algorithm is deciding which of these methods to use next and how large of a step-size Δp to use in the predictor [3, 12]. A trial-and-error approach for the step-size control is used for homotopy continuation tracking: shorten the step-size upon failure and lengthen it upon repeated successes [5, 42]. This trial-and-error approach can be computationally expensive and can lack efficiency when systems are not well-conditioned, since the step-size becomes

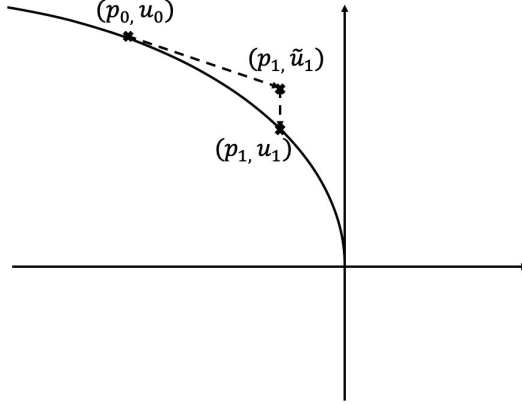


Figure 1: An illustration of the predictor-corrector Method.

very small. Moreover, in the path tracking process, at some critical points, the ill-conditioned Jacobian matrix $F_{\mathbf{u}}$ often causes trouble either in the prediction or in the correction process. Various computational techniques, such as pseudo-arclength continuation, Gauss-Newton continuation, and other adaptive step-size strategies [12], have been developed to handle this difficulty. For instance, the path tracking may encounter no difficulty at a turning point if the pseudo-arclength continuation is adopted. However, bifurcations of large-scale nonlinear systems are usually complex (more than turning points) and need a more sophisticated numerical method to compute.

3 Adaptive Homotopy Tracking with Bifurcation Detection (AHTBD)

To overcome this difficulty, an adaptive homotopy tracker is proposed to reduce the computational cost. The basic idea of this adaptive homotopy tracker is to solve the step-size simultaneously when we track the nonlinear system. For any given step-size h , we start with a point on the solution path, denoted by (\mathbf{u}_0, p_0) , and want to find the next point to satisfy the following augmented system:

$$\tilde{\mathbf{F}}(\mathbf{u}, p) = \begin{pmatrix} \mathbf{F}(\mathbf{u}, p) \\ g\mathbf{v}^T(\mathbf{u} - \mathbf{u}_0)(1 - s) + s(p - p_0) - h \end{pmatrix}, \quad (2)$$

where $g = \text{sign}(-\mathbf{v}^T \mathbf{F}_{\mathbf{u}}(\mathbf{u}_0, p_0)^{-1} \mathbf{F}_p(\mathbf{u}_0, p_0)) / \|\mathbf{F}_{\mathbf{u}}(\tilde{\mathbf{u}}, \tilde{p})^{-1} \mathbf{F}_p(\tilde{\mathbf{u}}, \tilde{p})\|$, $s = \left| \frac{\lambda_{\min}}{\tilde{\lambda}_{\min}} \right|$, λ_{\min} is the real part of the minimum eigenvalue of $\mathbf{F}_{\mathbf{u}}$ at (\mathbf{u}_0, p_0) , and \mathbf{v} is the corresponding eigenvector. Here $(\tilde{\mathbf{u}}, \tilde{p})$ is a generic point (i.e., randomly choosing \tilde{p} to compute $\tilde{\mathbf{u}}$) [5, 42] and $\tilde{\lambda}_{\min}$ is the real part of the minimum eigenvalue of $\mathbf{F}_{\mathbf{u}}$ at \tilde{p} . Thus the next point on the path (\mathbf{u}, p) is computed by solving the new augmented system \tilde{F} with an adaptive step-size. In particular, when the tracking parameter p is close to a bifurcation point, λ_{\min} is very small, and s approaches zero, we then have $g\mathbf{v}^T(\mathbf{u} - \mathbf{u}_0) = h$ instead of $p - p_0 = h$ which means that we change the tracking parameter from p to $\mathbf{v}^T \mathbf{u}$; when p_0 is a generic point, namely, the original system is well-conditioned, we have s be close to 1 and then $p = p_0 + h$ which is the “initial” target for the next point. Moreover, this adaptive homotopy tracking process, whose pseudocode is outlined in **Algorithm 1**, employs the Newton-Krylov method to solve the augmented nonlinear system.

Algorithm 1: The pseudocode of the adaptive tracking algorithm.

Input: A step-size h , a start point (\mathbf{u}_0, p_0) , and an ending parameter p_e
Output: A solution sequence on the path $(\mathbf{u}_i, p_i)_{i=1}^N$
Set $i = 0$;
while $(p - p_0)(p - p_e) \leq 0$ **do**
 Compute the minimum eigenvalue of $\mathbf{F}_{\mathbf{u}}(\mathbf{u}_i, p_i)$ and the corresponding eigenvector, \mathbf{v} ;
 Solve the augmented system (2) and denote the solution as $(\mathbf{u}_{i+1}, p_{i+1})$;
 Set $i = i + 1$;
end

Remark 1: The augmented system (2) does not bring new singularities. In other words, if the original system is full rank, then the augmented system must be full rank. In fact, if $\mathbf{F}_{\mathbf{u}}$ is not singular, the Jacobian matrix of the augmented system (2) can be written as

$$\begin{pmatrix} \mathbf{F}_{\mathbf{u}} & \mathbf{F}_p \\ g\mathbf{v}^T(1-s) & s \end{pmatrix} = \begin{pmatrix} I & 0 \\ g\mathbf{v}^T(1-s)\mathbf{F}_{\mathbf{u}}^{-1} & I \end{pmatrix} \begin{pmatrix} \mathbf{F}_{\mathbf{u}} & \mathbf{F}_p \\ 0 & s - g\mathbf{v}^T(1-s)\mathbf{F}_{\mathbf{u}}^{-1}\mathbf{F}_p \end{pmatrix}.$$

If the original system has full rank, namely, $s \neq 0$, then we have $s - (1-s)g\mathbf{v}^T\mathbf{F}_{\mathbf{u}}^{-1}\mathbf{F}_p \neq 0$, which implies that the augmented system (2) also has full rank. On the other hand, if F_u is singular, the Jacobian matrix of the augmented system could be non-singular.

Remark 2: The parameter tracking direction is the same as h . In fact, by solving

$$\begin{pmatrix} \mathbf{F}_{\mathbf{u}} & \mathbf{F}_p \\ g\mathbf{v}^T(1-s) & s \end{pmatrix} \begin{pmatrix} \Delta \mathbf{u} \\ \Delta p \end{pmatrix} = \begin{pmatrix} 0 \\ h \end{pmatrix},$$

we have

$$\Delta p = \frac{h}{s - (1-s)g\mathbf{v}^T\mathbf{F}_{\mathbf{u}}^{-1}\mathbf{F}_p}.$$

Noticing the definition of g , we have $s - (1-s)g\mathbf{v}^T\mathbf{F}_{\mathbf{u}}^{-1}\mathbf{F}_p > 0$ if $s \neq 0$, which implies that Δp has the same sign as h .

3.1 Inflation Process

When the Jacobian matrix of the augmented system is ill-conditioned, the adaptive path tracking algorithm based on Newton's method is no longer satisfactory since it may converge slowly or even diverge. Once such a circumstance occurs, the deflation technique has been proposed to overcome this difficulty [34, 27]. However, the deflated system is double the size of the original nonlinear system, and sometimes even higher order derivatives need to be taken into consideration [34]. Therefore this technique is hard to apply for large-scale systems. In order to track large-scale systems, we need a different strategy, an inflation process. The motivation of the inflation technique is based on iterative methods for the ill-conditioned symmetric positive definite matrices. Let us consider a simple example with $(A + \epsilon I)x = b$ (A and b are shown below), and apply the Gauss-Seidel method with stopping criteria $\|Ax^k - b\| \leq 10^{-8}$ and $x^0 = b$. Eq. (3) shows the number of iterations for different value of ϵ : the number of iterations increases dramatically from 18 to 54,470 when the matrix is ill-conditioned; the number of iterations drops to 2 when the matrix is singular. Therefore iterative methods usually are effective for a singular system, but time-consuming for a nearly singular system (see [33] for more theoretical results).

$$A = \begin{bmatrix} 1 & -1 & 0 \\ -1 & 2 & -1 \\ 0 & -1 & 1 \end{bmatrix}, b = \begin{bmatrix} -1 \\ -1 \\ 2 \end{bmatrix} \in R(A). \quad (3)$$

ϵ	# of iteration
1	18
10^{-1}	100
10^{-2}	852
10^{-3}	6,982
10^{-4}	54,470
0	2

Based on this motivation, we will inflate the nearly singular system to a singular system. More specifically, for a bifurcation point p^* , the system $\mathbf{F}(\mathbf{u}^*, p^*)$ is singular. By denoting J the Jacobian $\mathbf{F}_{\mathbf{u}}(\mathbf{u}, p)$, we know that J is ill-conditioned if p is close to p^* so that Newton's method becomes difficult to converge. By decomposing $\Delta \mathbf{u}$ as $\Delta \mathbf{u} = \widetilde{\Delta \mathbf{u}} + \alpha \mathbf{v}$, then we solve the following inflated system instead of $\mathbf{F}_{\mathbf{u}}(\mathbf{u}, p)\Delta \mathbf{u} =$

$-\mathbf{F}(\mathbf{u}, p)$:

$$\begin{pmatrix} J^T J & J^T J \mathbf{v} \\ \mathbf{v}^T J^T J & \lambda_{min} \end{pmatrix} \begin{pmatrix} \widetilde{\Delta \mathbf{u}} \\ \alpha \end{pmatrix} = - \begin{pmatrix} J^T F(\mathbf{u}, p) \\ \mathbf{v}^T J^T F(\mathbf{u}, p) \end{pmatrix}. \quad (4)$$

Here λ_{min} is the eigenvalue of $J^T J$ with the minimum norm and \mathbf{v} is the corresponding eigenvector. We use $J^T J$ instead of J to make sure the coefficient matrix is symmetric positive semi-definite in order to guarantee the convergence of this inflation technique [33]. In fact, for any $a \in \mathbb{R}^{n \times 1}, b \in \mathbb{R}$, we have

$$\begin{aligned} (a^T, b) \begin{pmatrix} J^T J & J^T J \mathbf{v} \\ \mathbf{v}^T J^T J & \lambda_{min} \end{pmatrix} \begin{pmatrix} a \\ b \end{pmatrix} &= a^T J^T J a + b \mathbf{v}^T J^T J a + a^T J^T J \mathbf{v} b + \lambda_{min} b^2 \\ &= a^T J^T J a + 2\lambda_{min} b a^T \mathbf{v} + \lambda_{min} b^2 \\ &\geq \lambda_{min} |a|^2 - 2\lambda_{min} |b| |a| |\mathbf{v}| + \lambda_{min} b^2 \\ &\geq \lambda_{min} (|a| - |b|)^2, \end{aligned} \quad (5)$$

which implies that the matrix in (4) is symmetric positive semi-definite. Therefore linear iterative solvers such as Gauss-Seidel or GMRES [47, 48] converge very quickly for solving the singular inflated system (4) [33].

Remark: Since $(\mathbf{v}^T, -1)^T$ is in the kernel of (4), we have a family of solutions $(\widetilde{\Delta \mathbf{u}} + k\mathbf{v}, \alpha - k)$ for (4), $\forall k$, for any given solution pair $(\widetilde{\Delta \mathbf{u}}, \alpha)$. However $\Delta \mathbf{u}$ is unique for any k by the definition.

3.2 Puiseux Series Extrapolation

The power series endgame has been successfully used to handle the singularity in NAG [2, 39] for polynomial systems. This endgame technique is only used for homotopy tracking very near $t = 0$, but cannot handle the bifurcation point during the tracking. In this paper, we will develop a new numerical method based on the Puiseux Series Expansion (PSE) to approximate the bifurcation point and the solution at the bifurcation point when the nonlinear system is polynomial. The idea is to use the eigenvalue of the Jacobian matrix to interpolate the solution near the bifurcation point. In particular, at the bifurcation point, the Jacobian $\mathbf{F}_{\mathbf{u}}$ has an eigenvalue with zero real part, say p_b , and several branches can come together at (\mathbf{u}_b, p_b) . We denote $\lambda = \min_i |\text{real}(\lambda_i)|$, where λ_i is the eigenvalue of $\mathbf{F}_{\mathbf{u}}(\mathbf{u}, p)$ for any given (\mathbf{u}, p) . Then according to the classical Puiseux's theorem (Chapter 7 in [13] & Corollary A.3.3 in [42]) we use a Puiseux series expansion to approximate (\mathbf{u}, p) in a neighborhood of (\mathbf{u}_b, p_b) , called the PSE operating zone. Thus the following

formulation is given by

$$\mathbf{u}(\lambda) = \mathbf{u}_b + \sum_{j=1}^{\infty} \mathbf{a}_j \lambda^{j/c_1} \text{ and } p(\lambda) = p_b + \sum_{j=1}^{\infty} b_j \lambda^{j/c_2}, \quad (6)$$

where c_1 and c_2 are the winding numbers for path $\mathbf{u}(\lambda)$ and $p(\lambda)$, respectively. Computing the winding numbers c_1 and c_2 requires more advanced computational techniques in NAG [5, 29, 42] but can not be applied directly for large-scale nonlinear systems, e.g., the discretized polynomial systems of nonlinear PDEs. Thus in our algorithm, we make several guesses at c_1 and c_2 to get the close connection to the curvature of the paths.

Moreover, we also need to compute leading terms of the PSE, namely, $w = \min\{j | \mathbf{a}_j \neq 0\}$ and $q = \min\{j | b_j \neq 0\}$. Then (6) is rewritten as

$$\mathbf{u}(\lambda) = \mathbf{u}_b + \lambda^{w/c_1} (\mathbf{a}_w + \sum_{j=w+1}^{\infty} \mathbf{a}_j \lambda^{j/c_1}) \text{ and } p(\lambda) = p_b + \lambda^{q/c_2} (b_q + \sum_{j=q+1}^{\infty} b_j \lambda^{j/c_2}). \quad (7)$$

We will show the procedure how to estimate q/c_2 , which can be extended to estimate w/c_1 as well: for any constant k_1 and k_2 , we have

$$\begin{aligned} p(k_1 \lambda) &= p_b + k_1^{q/c_2} \lambda^{q/c_2} (b_q + \sum_{j=q+1}^{\infty} b_j (k_1 \lambda)^{j/c_2}), \\ p(k_2 \lambda) &= p_b + k_2^{q/c_2} \lambda^{q/c_2} (b_q + \sum_{j=q+1}^{\infty} b_j (k_2 \lambda)^{j/c_2}). \end{aligned}$$

When λ is small and $k_1 < 1, k_2 < 1$, we have

$$\frac{1 - k_1^{q/c_2}}{1 - k_2^{q/c_2}} \approx \frac{p(\lambda) - p(k_1 \lambda)}{p(\lambda) - p(k_2 \lambda)}.$$

Thus an approximation of q/c_2 is obtained by solving the following nonlinear equation:

$$f(x) := 1 - k_1^x - m(1 - k_2^x) = 0,$$

where $m = \frac{p(\lambda) - p(k_1 \lambda)}{p(\lambda) - p(k_2 \lambda)}$. For estimating w/c_1 , we multiply a random vector, α , namely, using $\alpha^T \mathbf{u}(k_1 \lambda)$ and $\alpha^T \mathbf{u}(k_2 \lambda)$ to repeat the above procedure. In summary, the

algorithm for computing the bifurcation point based on the PSE is as follows:

Algorithm 2: Implementing PSE

Given a sequence of points on the branch, say $(\mathbf{u}^n, p^n, \lambda^n)_{n=1}^N$;
while $|\lambda| < Tol$ **do**
 Estimate the value of w/c_1 and q/c_2 by solving the nonlinear equation
 $f(x) = 0$;
 for $c_i = 1 : M$ **do**
 Use the first $N - 1$ points to approximate the Puiseux series;
 Apply these approximations to extrapolate (\mathbf{u}^N, p^N) at λ^N ;
 end
 Determine the best value of c_i by choosing the nearest extrapolating point
 on the paths at $\lambda = \lambda^N$;
 Use the Puiseux series to approximate (\mathbf{u}_b, p_b) at $\lambda = 0$;
 if $\|F(\mathbf{u}_b, p_b)\| < Tol$ **then**
 | Break;
 else
 Set $\lambda = \frac{\lambda_N}{2}$, generate a new point $(\mathbf{u}^{N+1}, p^{N+1})$, and update the
 sequence of points;
 end
end

An illustrated example: We will use the following example to illustrate this PSE interpolation process:

$$F(\mathbf{u}, p) = \begin{pmatrix} x^2 - p^2 \\ (x + y)^2 - p^3 \end{pmatrix}. \quad (8)$$

In this example, exact solutions of one branch are

$$x = -\left(\frac{1}{2}\right)^{2/3} \lambda^{2/3}, \quad y = \left(\frac{1}{2}\right)^{1/3} \lambda^{2/3} + \frac{1}{2} \lambda \quad \text{and} \quad p = \left(\frac{1}{2}\right)^{2/3} \lambda^{2/3},$$

where λ is the minimum eigenvalue of the Jacobian matrix. By taking $\lambda = 2$, we have our initial point $x_0 = -1$, $y_0 = 2$, and $p_0 = 1$. By taking $h = -0.1$, we collect five points on this solution path shown in Fig. 2. Four of them are used to compute coefficients of the Puiseux series, the other one is to determine the winding numbers c_1 and c_2 . Fig. 2 shows different solution trajectories by using PSE interpolation for different c_1 . Then $c_1 = 3$ is the best approximation for x , y . In fact, since p is a monomial of λ , when using a different winding number c_2 , the ratio q/c_2 is the same. Then the approximated bifurcation point becomes $x = -3.2 \times 10^{-5}$, $y = 1.1 \times 10^{-4}$, and $p = 3.2 \times 10^{-5}$.

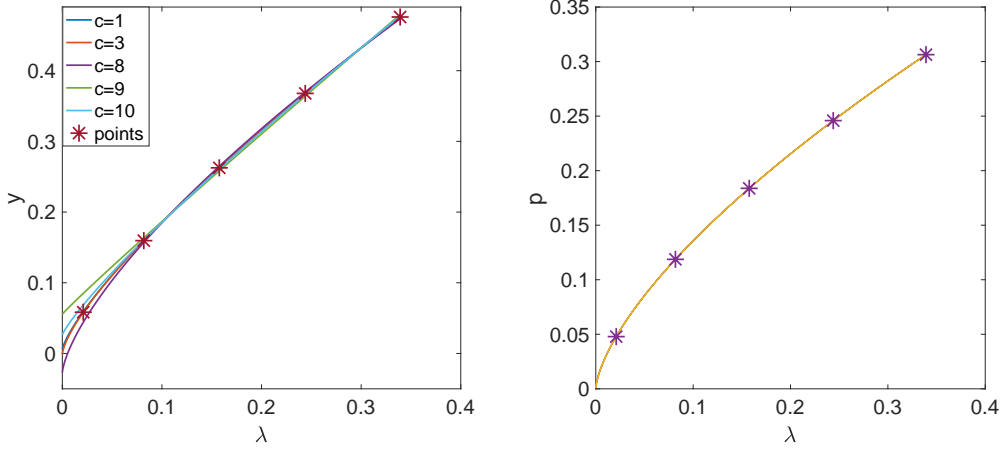


Figure 2: The PSE interpolation in the illustrated example (8). The left part shows solution trajectories of y with respect to λ for different c_1 ; the right part shows parameter p with respect to λ .

3.3 Tangent Cone

After computing the bifurcation point, the tangent cone of the bifurcation point needs to be computed in order to track along different branches by using the Lyapunov-Schmidt reduction [7, 9, 21]. The tangent cone T_* and the Jacobian matrix J_* at the bifurcation point have the following relationship

$$T_* \subseteq \text{null}(J_*),$$

which implies that the tangent cone is contained in the tangent space at a bifurcation although the tangent cone and tangent space are equal at a generic point. Then the null space of the Jacobian is computed to obtain the tangent cone at a bifurcation by using the Taylor expansion of the nonlinear system \mathbf{F} in the null space of J_* . We will illustrate the procedure of computing the tangent cone by assuming that the dimension of the null space of the J_* is $n - 1$. Let's denote the Jacobian $J_{\mathbf{u}}$ and the derivative J_p with respect to p at (\mathbf{u}_0, p_0) as $A := [J_{\mathbf{u}}, J_p] \in R^{n \times (n+1)}$. Then we have

$$\begin{bmatrix} \mathbf{Q}_1 & \mathbf{Q}_2 \\ q_1 & q_2 \end{bmatrix} = \text{null}(A), \text{ where } \mathbf{Q}_i \in R^{n \times 1} \text{ and } q_i \text{ is a scalar.}$$

Similarly, $\Lambda \in R^{1 \times n} = \text{null}(A^T)$. Thus we assume that

$$\Delta \mathbf{u} = a_1 \mathbf{Q}_1 + a_2 \mathbf{Q}_2 \text{ and } \Delta p = a_1 q_1 + a_2 q_2,$$

where a_i needs to be determined. We construct the following single polynomial $g(a_1, a_2)$

$$g(\mathbf{a}) = \Lambda^T F(\mathbf{u}_0 + a_1 \mathbf{Q}_1 + a_2 \mathbf{Q}_2, p_0 + a_1 q_1 + a_2 q_2).$$

By using Taylor expansion at $(0, 0)$, we have

$$g(\mathbf{a}) \approx g(0, 0) + \mathbf{a}^T \frac{\partial g}{\partial \mathbf{a}}(0, 0) + \frac{1}{2} \mathbf{a}^T H(0, 0) \mathbf{a},$$

where $H(0, 0)$ is the Hessian matrix of g at $(0, 0)$. Then \mathbf{a} stratifies the following system:

$$\begin{aligned} \mathbf{a}^T H(\mathbf{0}) \mathbf{a} &= 0 \\ a_1 q_1 + a_2 q_2 &= \Delta_p. \end{aligned}$$

If the tangent cone has a more complex structure (such as when the dimension of the null space of the Jacobian is more than 1), we need to introduce more variables a_i and more derivatives to determine the tangent cone.

Therefore, we summarize the AHTBD method as follows and outline the flow chart in Fig. 3:

1. For a given initial point (\mathbf{u}, p) on a solution path and a maximum step-size, solve the augmented system (2) to track along the path;
2. If the augmented system (2) becomes ill-conditioned, the inflation process is introduced;
3. Near the bifurcation point, the PSE interpolation is used to approximate the bifurcation point;
4. At the bifurcation point, the tangent cone is computed to determine the different tracking solution branches, and then repeat the first step for each path.

4 Numerical Results

In this section, we apply the AHTBD method to several examples, ranging from a single equation to a system of nonlinear PDEs, to show its efficiency. Both the AHTBD method and the traditional homotopy tracking method are implemented and compared on Matlab. The traditional homotopy tracking has been implemented in various packages such as Bertini [3], HOM4PS [32], PHCpack [44] and others to handle the bifurcations. Among these existing software, Bertini has more freedom to

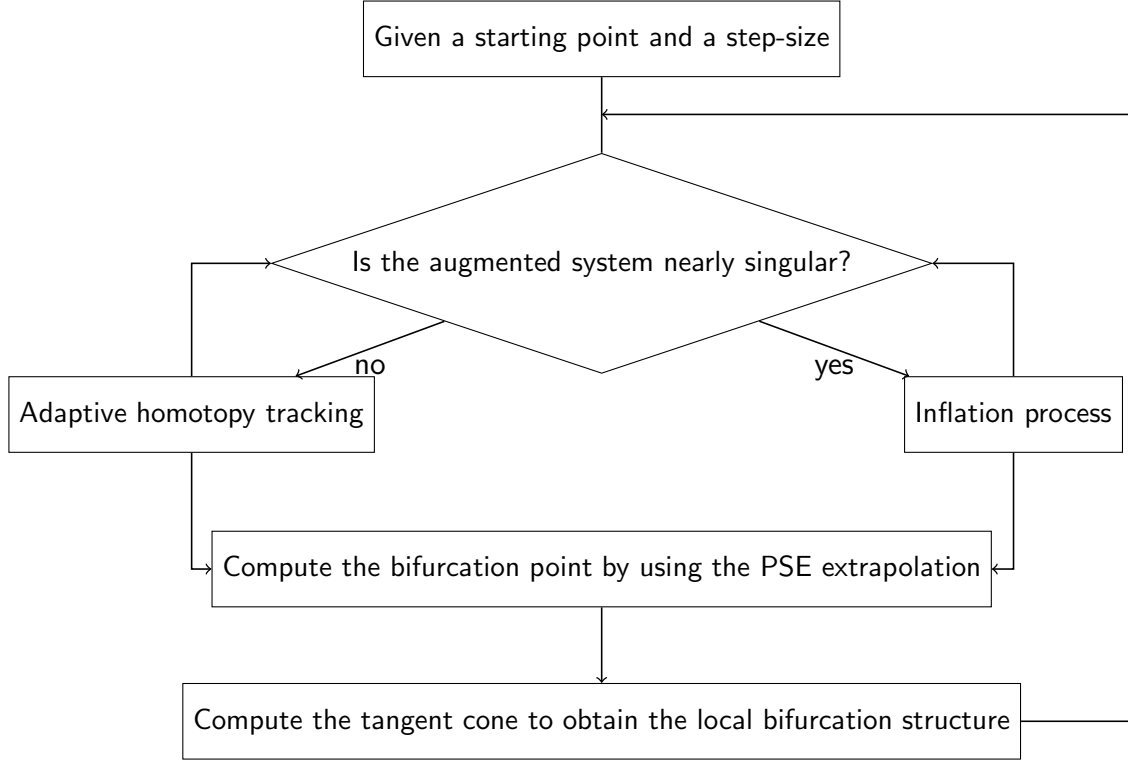


Figure 3: The flow chart of the AHTBD method.

compute the bifurcations due to the adaptive multi-precision path tracking [4] and the parallel endgame [6]. To fairly compare the AHTBD method with the traditional homotopy tracking, we will implement both methods on Matlab.

4.1 An example with a turning point

Our first example is used to test the efficiency of adaptive homotopy tracker by considering the following system:

$$F(\mathbf{u}, p) = \begin{pmatrix} x^2 - p \\ x^2 - 2y^2 + p \end{pmatrix}, \quad (9)$$

where $\mathbf{u} = (x, y)^T$ is the variable while p is the parameter. The analytical solution is $x^2 = y^2 = p$ which has a turning point when $p = 0$. This example is used to illustrate the efficiency of the adaptive homotopy tracker for computing the bifurcation point. We choose $\mathbf{u}_0 = (-1, 1)$ and $p_0 = 1$ as our initial tracking point and compare the

adaptive homotopy tracker of the AHTBD method and the traditional homotopy tracker with different step-sizes ($h = -0.1$ and $h = -0.2$). Table 1 and Fig. 4 show that the adaptive homotopy tracker takes fewer steps to get to the bifurcation point. In particular, when the initial step-size h becomes larger, the efficiency of the adaptive homotopy tracker is more obvious. The traditional homotopy method finds the bifurcation by halving the step-size with less accuracy (around 10^{-4}), while the adaptive homotopy tracker approximates the bifurcation point by doing the PSE extrapolation with higher accuracy (around 10^{-6}).

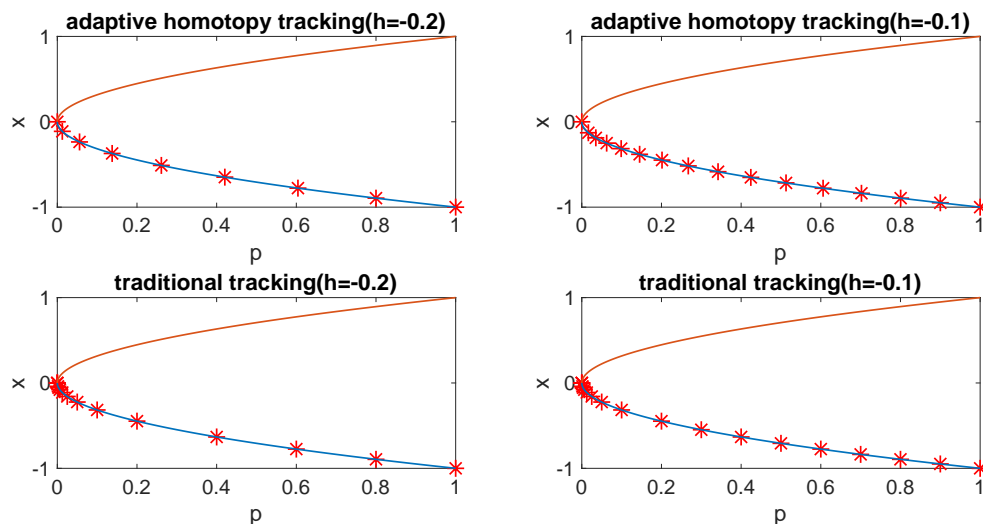


Figure 4: Comparisons between adaptive (upper) and traditional (lower) homotopy tracking methods. The plot of x v.s. p is illustrated for $h = -0.2$ (left) and $h = -0.1$ (right).

4.2 Examples with complex bifurcation structures

In this subsection, we will use the AHTBD method to compute several examples with complex bifurcation structures; namely, the bifurcation point is computed first by using the adaptive homotopy tracker, and then the tangent cone algorithm is used to obtain different solution branches.

Example 1: Given

$$F(x, p) = (x - p)^4 + (x - p)(x + p), \quad (10)$$

		h=-0.1		h=-0.2	
		traditional	adaptive	traditional	adaptive
# of steps		19	16	15	9
bifurcation	x	3×10^{-4}	-1.695×10^{-5}	3×10^{-4}	-1.1×10^{-16}
	y	-3×10^{-4}	1.695×10^{-5}	-3×10^{-4}	1.1×10^{-16}
	p	-5.7×10^{-7}	5.5×10^{-6}	-5.7×10^{-7}	3.8×10^{-11}

Table 1: Comparisons between adaptive and traditional homotopy tracking methods for (9).

we have a bifurcation point at $p = 0$. In order to compute the local bifurcation diagram at $p = 0$, we start from a point $x = 1$ and $p = 1$ to track along a solution path with the step-size $h = -0.1$. When it is close to the bifurcation, namely, $\lambda_{min} < 0.1$, we use the PSE to approximate the bifurcation point. Afterwards the tangent cone is computed: since the Jacobian F_x and the derivative F_p are both 0, the null space for $A = [F_x, F_p]$ is $\text{span}\{(0, 1)^T, (1, 0)^T\}$ and the null space of A^T is $\text{span}\{1\}$. Then two tangent directions are obtained, $(1, 1)^T$ and $(-1, 1)^T$. By setting different step-sizes, for example $h = \pm 0.1$, and choosing a tangent direction, we obtain a solution on each branch. Starting from this point, the adaptive homotopy algorithm is employed to continue tracking (see Fig. 5).

Example 2: The following equation represents two intersecting circles that imply complex bifurcation structures shown in Fig. 6:

$$F(x, p) = (x^2 + p^2 - 1)((x - 1)^2 + p^2 - 1). \quad (11)$$

We start to track along a solution path from point $(\frac{1}{2}, \frac{\sqrt{3}}{2})$ with different tracking directions (blue point in Fig. 6). Fig. 6 shows the AHTBD tracking process with the step-size $|h| = 0.1$. It is clearly seen that the tracking is almost uniform even though there are two bifurcation points. Table 2 shows the comparison between the AHTBD and traditional homotopy methods when the tracking starts at point $(\frac{1}{2}, \frac{\sqrt{3}}{2})$ and ends when reaching or passing the turning point where $|p| = 1$. The two tables have the same starting point, while the tracking direction is different. Although the traditional homotopy method may have higher accuracy for the bifurcation point, it takes many more steps to reach the end point than the AHTBD method. Moreover, the AHTBD method can pass the turning point easily (see Table 2 for $h = -0.1$), while the traditional method stagnates at the turning point.

Example 3: We consider the following equation which is used in [45] as an example

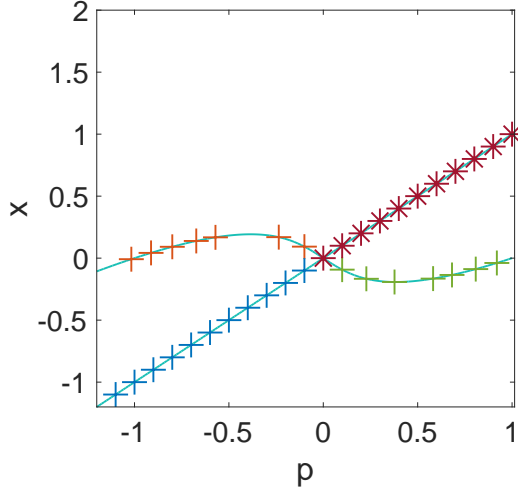


Figure 5: Local bifurcation diagram of (10): starting from the lower branch (blue points), we compute the bifurcation point first by using the PSE interpolation and then compute the tangent cone to obtain the other solution branches (green, red, and orange points).

of universal unfoldings of singularities of topological codimension two:

$$F(x, p) = (x - p)^2 + \left(\frac{1}{3} - 2(x + p) + (x + p)^3\right)(x - p). \quad (12)$$

We used the AHTBD method to track the solution branch starting from $(1, 1)$, which is shown as the blue point in Fig. 7 and is tracked along two different solution branches after the first bifurcation point. We also compared the traditional homotopy tracking with the AHTBD method on two branches: diagonal and non-diagonal (red and blue, respectively, in Fig. 7). In Table 3, we tracked from $(1, 1)$ with $h = -0.05$ until $p < -0.03$. When tracking along the non-diagonal branch, we encountered turning points where the AHTBD method works well. However, for the traditional method, we have to switch the tracking parameter from p to x in order to ensure the tracking process follows the correct direction.

		h=0.1		h=0.05	
		Trial-and-error	AHTBD	Trial-and-error	AHTBD
# of steps		50	10	60	17
bifurcation	x	0.5002	0.5020	0.5002	0.5033
	p	0.8659	0.8671	0.8659	0.8702
endpoint	x	0.0128	-0.2097	0.0128	-0.1020
	p	0.9999	0.9778	0.9999	0.9948
		h=-0.1		h=-0.05	
		Trial-and-error	AHTBD	Trial-and-error	AHTBD
# of steps		62	19	82	32
bifurcation	x	0.5002	0.5026	0.5002	0.4831
	p	-0.8659	-0.8675	-0.8659	-0.8756
endpoint	x	0.0080	-0.1637	0.0080	0.0054
	p	-1.0000	-0.9865	1.0000	-1.0000

Table 2: Comparisons between AHTBD and traditional trial-and-error tracking methods along the branches shown in Fig. 6 with different step-sizes for h .

		Diagonal branch		Non-diagonal branch	
		Trial-and-error	AHTBD	Trial-and-error	AHTBD
# of steps		139	27	273	60
1st bifurcation	x	0.6612	0.6609	0.6612	0.6609
	p	0.6612	0.6609	0.6612	0.6609
2nd bifurcation	x	0.0846	0.0873	0.0852	0.0860
	p	0.0846	0.0837	0.0843	0.0843

Table 3: Comparisons between AHTBD and traditional homotopy tracking methods for (12) along two branches.

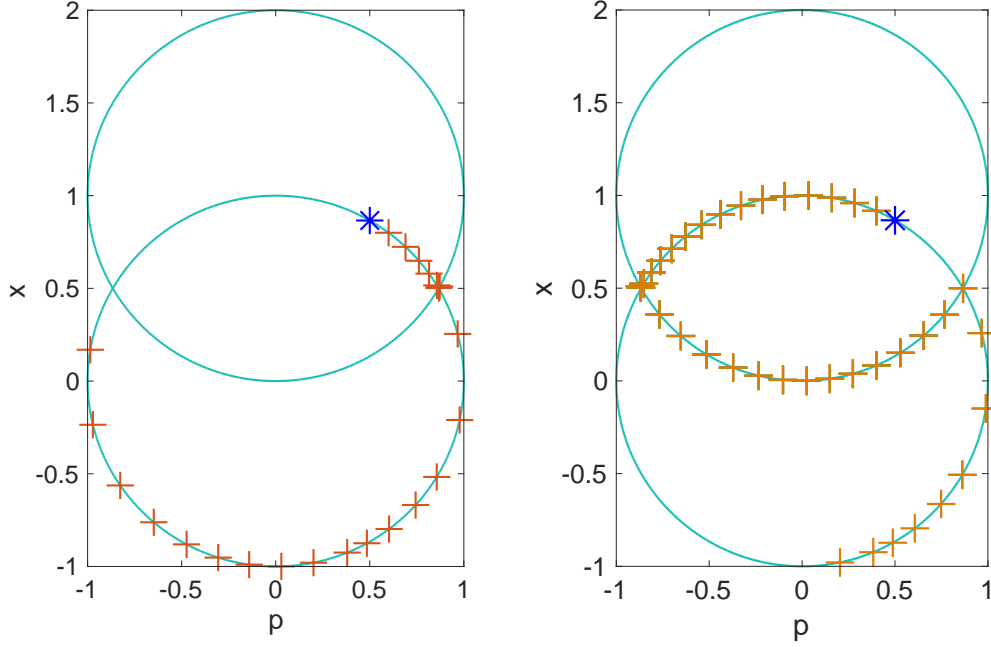


Figure 6: Local bifurcation diagram of (11). The AHTBD method is used to track from the blue point to the left and right directions.

4.3 An example of nonlinear PDEs

We compared the AHTBD method with the trial-and-error tracking method on the following nonlinear differential equation:

$$\begin{cases} u_{xx} = u^2(u^2 - p), \\ u_x(0) = 0, u(1) = 0, \end{cases}$$

where u is the solution of differential equation and p is the parameter. There are multiple solutions u for any given parameter p , moreover, the number of solutions increases as p goes large. We discretized the differential equation by using the finite difference method and obtained a nonlinear system of polynomial equations. For $p = 18$, we solved the discretized nonlinear system by using Newton's method with different initial guesses and obtained seven solutions that is shown in Fig. 8. Then we tracked p from 18 to 0 with $h = -0.4$ and compared two methods. The stopping criteria for the trial-and-error method is that the stepsize is less than $1e - 9$ while it is $p(p - 18) > 0$ for the AHTBD method. We compared two methods in the

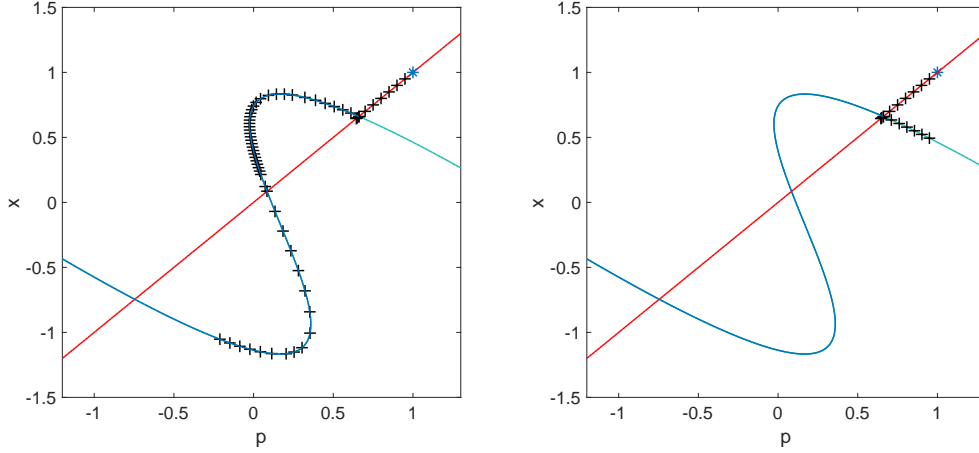


Figure 7: Solution behavior of (12) with diagonal (red) and non-diagonal (blue) branches.

tracking steps and running time for the nonlinear system with 360 grid points in Table 4. The AHTBD method is more efficient to obtain the full solution behaviors for different branches while the traditional trial-and-error tracking method obtains half of branches.

Branch No.	Trial-and-error		AHTBD	
	Steps	Elapsed time	Steps	Elapsed time
2	46 steps	1.1317s	31 steps	1.553s
3	57 steps	2.2933s	38 steps	1.7895s
4	33 steps	1.6764s	15 steps	0.7928s
5	30 steps	1.6732s	16 steps	0.8745s

Table 4: Comparisons between the AHTBD method and the trial-and-error method for the discretized nonlinear system of (4.3) with 360 grid points.

5 Application to a system of nonlinear PDEs

We apply the AHTBD method to a system of nonlinear PDEs to model two species: consider a competition between two species that are ecologically identical except in their dispersal mechanisms. Let $u = u(x)$, $v = v(x)$ denote the densities of two competing species at location x . Then the study of the interaction between a resident

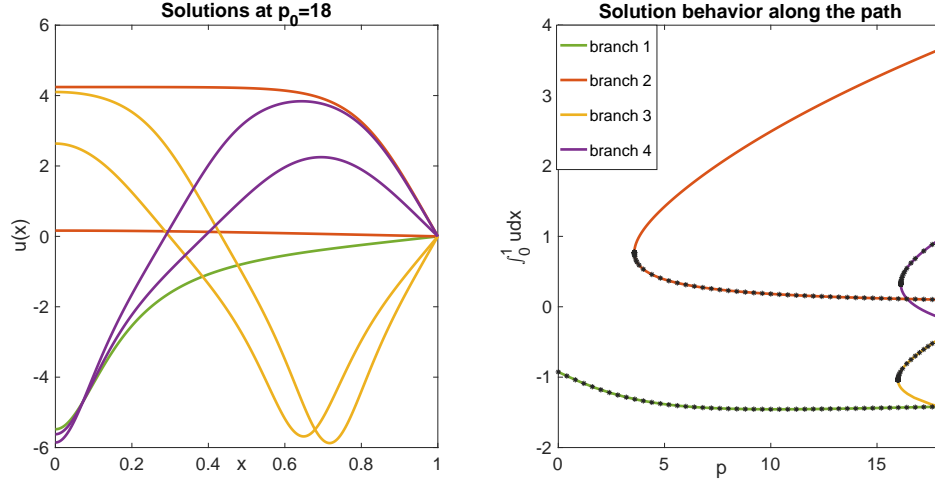


Figure 8: **Left:** Non-trivial solutions of (4.3) at $p_0 = 18$; **Right:** Solution behavior of (4.3) obtained by both the AHTBD method(solid line) and the traditional method(asterisk).

phenotype (u) with an invader phenotype (v) can be modeled by the following system:

$$\begin{cases} \nabla(d\nabla u - \alpha u \nabla m) &= -u(m - u) & \text{in } \Omega, \\ \nabla(d\nabla v - \beta v \nabla m) &= -v(m - u) & \text{in } \Omega, \\ d\frac{\partial u}{\partial n} - \alpha u \frac{\partial m}{\partial n} &= d\frac{\partial v}{\partial n} - \beta v \frac{\partial m}{\partial n} = 0 & \text{on } \partial\Omega. \end{cases} \quad (13)$$

Here $m(x)$ is the per-capita growth rate, which represents the same resources that two species are competing for. To reflect the heterogeneity of the environment, we assume that $m(x)$ is a nonconstant function to reflect the quality and quantity of resources available at the location x . In Eq. (13), d is two species' common random dispersal rates, and α, β are their rates of directed movement upward along the resource gradient. The boundary condition is of a no-flux type, i.e., there is no net movement across the boundary. The solution behavior of this model has been studied well in [8, 18, 24, 31]: when $\alpha = \beta$, two species co-exist, $u = v$. Bifurcation, the so-called evolutionarily stable strategy (ESS), happens on the diagonal $\alpha = \beta$, and the behavior of the solution near the bifurcation point is described in [8, 18, 31]. In reality, it is interesting to find out what happens for the bifurcation branch away from the bifurcation point, and this is where the numerical computation is needed: to find the population densities u and v as α and β moves far away from the ESS. Given $m(x) = 1 + x$, a unique positive solution of u is defined by (13), namely,

$\tilde{u} = \tilde{u}(d, \alpha)$. By standard theory, if some rare population v is introduced into the resident population u at equilibrium (i.e. $u \equiv \tilde{u}$), then the initial (exponential) growth rate of the population of v is given by λ , where $\lambda = \lambda(\alpha, \beta; d)$ is the principal eigenvalue of the problem

$$\begin{cases} \nabla \cdot (d \nabla \varphi - \beta \varphi \nabla m) + (m - \tilde{u}(d, \alpha)) \varphi = \lambda \varphi & \text{in } \Omega, \\ d \frac{\partial \varphi}{\partial n} - \beta \varphi \frac{\partial m}{\partial n} = 0 & \text{on } \partial \Omega, \end{cases} \quad (14)$$

where the positive principal eigenfunction $\varphi = \varphi(\alpha, \beta; d)$ is uniquely determined by the normalization

$$\int_{\Omega} \varphi(\alpha, \beta; d) = 1. \quad (15)$$

In particular, when $\alpha = \beta$, we have $\varphi(\alpha, \alpha; d) = \tilde{u}$ and $\lambda(\alpha, \alpha; d) \equiv 0$ for any d, α which implies that two species u and v are identical when $\alpha = \beta$.

When we couple (13) and (15) together and discretize the system by using the finite difference method, we have the following coupled system:

$$\mathbf{F}(\beta, \mathbf{u}, \mathbf{v}; \alpha) := \begin{pmatrix} \frac{2d}{h^2} u_2 - (\frac{2d}{h^2} + \frac{2\alpha}{h} + \frac{\alpha^2}{d}) u_1 + u_1(m_1 - u_1) \\ \frac{d}{h^2}(u_{i+1} - 2u_i + u_{i-1}) - \frac{\alpha}{2h}(u_{i+1} - u_{i-1}) + u_i(m_i - u_i) \\ (-\frac{2d}{h^2} + \frac{2\alpha}{h} - \frac{\alpha^2}{d}) u_N + \frac{2d}{h^2} u_{N-1} + u_N(m_N - u_N) \\ \frac{2d}{h^2} v_2 - (\frac{2d}{h^2} + \frac{2\beta}{h} + \frac{\beta^2}{d}) v_1 + v_1(m_1 - u_1) \\ \frac{d}{h^2}(v_{i+1} - 2v_i + v_{i-1}) - \frac{\beta}{2h}(v_{i+1} - v_{i-1}) + v_i(m_i - u_i) \\ (-\frac{2d}{h^2} + \frac{2\beta}{h} - \frac{\beta^2}{d}) v_N + \frac{2d}{h^2} v_{N-1} + v_N(m_N - u_N) \\ (\frac{v_1}{2} + v_2 + \dots + v_{N-1} + \frac{v_N}{2})h - 1 \end{pmatrix} = 0. \quad (16)$$

For any given α_0 , \mathbf{u}_0 is solved by the discretization of (13). Then $\mathbf{u}_0, \beta_0 = \alpha_0, \mathbf{v}_0 = \frac{\mathbf{u}_0}{\int_{\Omega} \mathbf{u}_0}$ is a solution of $\mathbf{F}(\beta, \mathbf{u}, \mathbf{v}; \alpha) = 0$. Given initial values $(\beta_0, \mathbf{u}_0, \mathbf{v}_0, \alpha_0)$, we track along the diagonal branch $\alpha = \beta$ using α as a parameter. For our choice of $m(x)$, there is only one bifurcation. We applied the AHTBD method to track $\mathbf{F}(\beta, \mathbf{u}, \mathbf{v}; \alpha) = 0$, which is shown in Fig. 9 by starting with $\alpha_0 = 0.01$ and ending with $\alpha_0 > 0.3$. We also compared the AHTBD method with the traditional trial-and-error tracking method in Tables 5 & 6 and demonstrated that the AHTBD method is faster than the traditional homotopy tracking method for the nonlinear PDE example.

6 Conclusions

We developed an adaptive homotopy tracking method to compute bifurcations for large-scale nonlinear parametric systems. This new algorithm is designed for comput-

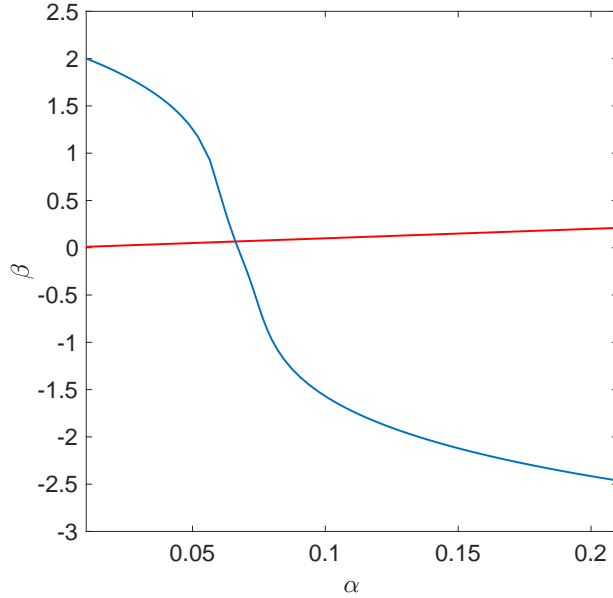


Figure 9: Diagram of α - β by tracking $\mathbf{F}(\beta, \mathbf{u}, \mathbf{v}; \alpha) = 0$ with respect to α .

ing bifurcation points and solutions on different branches through the bifurcations via adaptive tracking, the Puiseux interpolation, and the inflation process. Furthermore, an augmented system is introduced to compute the adaptive parameter step-size while the inflation technique is backed up when the augmented system becomes singular. We also employ the Puiseux series expansion to interpolate bifurcation points, and different bifurcation branches are approximated based on computing the tangent cone structure of the bifurcation point. Several numerical examples for both polynomial systems and nonlinear systems of PDEs verify the efficiency of this new method through comparison with the traditional homotopy continuation method. There are still some numerical challenges for the adaptive homotopy tracking method developed in this paper. For example, it would become challenging and might fail when we deal with a cluster of bifurcations. Moreover, the efficient and accurate eigenvalue solver is required in this adaptive tracking process. Thus inexact approximations of eigen data and inaccurate solution points might also affect the numerical performance. We will explore these challenges more carefully in the future.

h	Diagonal branch		Non-diagonal branch	
	Trial-and-error	AHTBD	Trial-and-error	AHTBD
0.01	88 steps(42.2808s)	25 steps(15.5970s)	88 steps(48.5956s)	26 steps(16.9497s)
0.02	70 steps(33.2463s)	16 steps(10.8033s)	70 steps(40.5963s)	15 steps(10.2496s)

Table 5: Comparison between the AHTBD method and the traditional trial-and-error tracking with different step-sizes for h (the number of grid points $N = 320$).

N	Diagonal branch		Non-diagonal lower branch	
	Trial-and-error tracking	AHTBD	Trial-and-error tracking	AHTBD
80	85 steps(5.7142s)	28 steps(2.7299s)	85 steps(6.1369s)	26 steps(2.4906s)
160	96 steps(17.9011s)	29 steps(6.2515s)	96 steps(19.1336s)	28 steps(6.6682s)
320	88 steps(42.2808s)	25 steps(15.5970s)	88 steps(48.5956s)	26 steps(16.9497s)

Table 6: Comparison between the AHTBD method and the traditional trial-and-error tracking for number of grid points N (the step-size is $h = 0.01$).

References

- [1] Eugene L Allgower and Kurt Georg. *Introduction to numerical continuation methods*, volume 45. SIAM, 2003.
- [2] D. Bates, J. Hauenstein, and A. Sommese. Efficient path tracking methods. *Numerical Algorithms*, 58(4):451–459, 2011.
- [3] D. Bates, J. Hauenstein, A. Sommese, and C. Wampler. Bertini: Software for numerical algebraic geometry, 2006.
- [4] D. Bates, J. Hauenstein, A. Sommese, and C. Wampler. Adaptive multiprecision path tracking. *SIAM Journal on Numerical Analysis*, 46(2):722–746, 2008.
- [5] D. Bates, J. Hauenstein, A. Sommese, and C. Wampler. *Numerically solving polynomial systems with Bertini*, volume 25. SIAM, 2013.
- [6] J. Bates, D. and Hauenstein and A. Sommese. A parallel endgame. *Contemp. Math*, 556:25–35, 2011.
- [7] Boris Buffoni, John Toland, and John Francis Toland. *Analytic theory of global bifurcation: an introduction*. Princeton University Press, 2003.

- [8] X. Chen, R. Hambrock, and Y. Lou. Evolution of conditional dispersal: a reaction-diffusion-advection model. *J Math Biol*, 57(3):361–386, 2008.
- [9] C. Chicone. Lyapunov-schmidt reduction and melnikov integrals for bifurcation of periodic solutions in coupled oscillators. *Journal of differential equations*, 112(2):407–447, 1994.
- [10] S. Choi, D. Harney, and N. Book. A robust path tracking algorithm for homotopy continuation. *Computers & chemical engineering*, 20(6):647–655, 1996.
- [11] B. Dayton and Z. Zeng. Computing the multiplicity structure in solving polynomial systems. In *Proceedings of the 2005 international symposium on Symbolic and algebraic computation*, pages 116–123. ACM, 2005.
- [12] Peter Deuffhard. *Newton methods for nonlinear problems: affine invariance and adaptive algorithms*, volume 35. Springer Science & Business Media, 2011.
- [13] G. Fischer. *Plane algebraic curves*, volume 15. American Mathematical Soc., 2001.
- [14] A. Friedman and W. Hao. A mathematical model of atherosclerosis with reverse cholesterol transport and associated risk factors. *Bulletin of mathematical biology*, 77(5):758–781, 2015.
- [15] A. Friedman and B. Hu. Bifurcation from stability to instability for a free boundary problem arising in a tumor model. *Archive for rational mechanics and analysis*, 180(2):293–330, 2006.
- [16] A. Friedman and B. Hu. Bifurcation for a free boundary problem modeling tumor growth by stokes equation. *SIAM Journal on Mathematical Analysis*, 39(1):174–194, 2007.
- [17] R. Haber and H. Unbehauen. Structure identification of nonlinear dynamic systems survey on input/output approaches. *Automatica*, 26(4):651–677, 1990.
- [18] R. Hambrock and Y. Lou. The evolution of conditional dispersal strategies in spatially heterogeneous habitats. *Bull. Math. Biol.*, 71(8):1793–1817, 2009.
- [19] W. Hao, E. Crouser, and A. Friedman. Mathematical model of sarcoidosis. *Proceedings of the National Academy of Sciences*, 111(45):16065–16070, 2014.
- [20] W. Hao and A. Friedman. The ldl-hdl profile determines the risk of atherosclerosis: a mathematical model. *PloS one*, 9(3):e90497, 2014.

- [21] W. Hao, J. Hauenstein, B. Hu, Y. Liu, A. Somme, and Y.-T. Zhang. Bifurcation for a free boundary problem modeling the growth of a tumor with a necrotic core. *Nonlinear Analysis: Real World Applications*, 13(2):694–709, 2012.
- [22] W. Hao, J. Hauenstein, B. Hu, and A. Somme. A three-dimensional steady-state tumor system. *Applied Mathematics and Computation*, 218(6):2661–2669, 2011.
- [23] W. Hao, J. Hauenstein, C.-W. Shu, A. Somme, Z. Xu, and Y.-T. Zhang. A homotopy method based on weno schemes for solving steady state problems of hyperbolic conservation laws. *Journal of Computational Physics*, 250(5):332–346, 2013.
- [24] W. Hao, K. Y. Lam, and Y. Lou. Concentration phenomena in an integro-pde model for evolution of conditional dispersal. *Indiana University Mathematics Journal*, page to appear, 2017.
- [25] W. Hao, R. Nepomechie, and A. Somme. Completeness of solutions of bethe’s equations. *Physical Review E*, 88(5):052113, 2013.
- [26] W. Hao, R. Nepomechie, and A. Somme. Singular solutions, repeated roots and completeness for higher-spin chains. *Journal of Statistical Mechanics: Theory and Experiment*, 2014(3):P03024, 2014.
- [27] J. Hauenstein and C. Wampler. Isosingular sets and deflation. *Foundations of Computational Mathematics*, 13(3):371–403, 2013.
- [28] T. Hou, J. Lowengrub, and M. Shelley. Boundary integral methods for multi-component fluids and multiphase materials. *Journal of Computational Physics*, 169(2):302–362, 2001.
- [29] B. Huber and J. Verschelde. Polyhedral end games for polynomial continuation. *Numerical Algorithms*, 18(1):91–108, 1998.
- [30] H. Khalil. Nonlinear systems. *Upper Saddle River*, 2002.
- [31] K. Y. Lam and Y. Lou. Evolution of conditional dispersal: evolutionarily stable strategies in spatial models. *J Math Biol*, 68(4):851–877, 2014.
- [32] T.-L. Lee, T.-Y. Li, and C.-H. Tsai. Hom4ps-2.0: a software package for solving polynomial systems by the polyhedral homotopy continuation method. *Computing*, 83(2):109–133, 2008.

- [33] Y. Lee, J. Wu, J. Xu, and L. Zikatanov. Robust subspace correction methods for nearly singular systems. *Mathematical Models and Methods in Applied Sciences*, 17(11):1937–1963, 2007.
- [34] A. Leykin, J. Verschelde, and A. Zhao. Newton’s method with deflation for isolated singularities of polynomial systems. *Theoretical Computer Science*, 359(1-3):111–122, 2006.
- [35] T.-Y. Li, T. Sauer, and J. Yorke. The cheater’s homotopy: an efficient procedure for solving systems of polynomial equations. *SIAM Journal on Numerical Analysis*, 26(5):1241–1251, 1989.
- [36] T.-Y. Li and Z. Zeng. Homotopy-determinant algorithm for solving nonsymmetric eigenvalue problems. *Mathematics of computation*, 59(200):483–502, 1992.
- [37] A. Morgan and A. Sommese. Computing all solutions to polynomial systems using homotopy continuation. *Applied Mathematics and Computation*, 24(2):115–138, 1987.
- [38] A. Morgan and A. Sommese. A homotopy for solving general polynomial systems that respects m-homogeneous structures. *Applied Mathematics and Computation*, 24(2):101–113, 1987.
- [39] A. Morgan, A. Sommese, and C. Wampler. A power series method for computing singular solutions to nonlinear analytic systems. *Numerische Mathematik*, 63(1):391–409, 1992.
- [40] P. Rabier and W. Rheinboldt. On a computational method for the second fundamental tensor and its application to bifurcation problems. *Numerische Mathematik*, 57(1):681–694, 1990.
- [41] W. Rheinboldt. Numerical methods for a class of finite dimensional bifurcation problems. *SIAM Journal on Numerical Analysis*, 15(1):1–11, 1978.
- [42] A. Sommese and C. Wampler. *The Numerical solution of systems of polynomials arising in engineering and science*, volume 99. World Scientific, 2005.
- [43] S. Strogatz. *Nonlinear dynamics and chaos: with applications to physics, biology, chemistry, and engineering*. Westview press, 2014.
- [44] J. Verschelde. Algorithm 795: Phcpack: A general-purpose solver for polynomial systems by homotopy continuation. *ACM Transactions on Mathematical Software (TOMS)*, 25(2):251–276, 1999.

- [45] X. Wang and M. Golubitsky. Singularity theory of fitness functions under dimorphism equivalence. *Journal of mathematical biology*, 73(3):525–573, 2016.
- [46] L. Watson, S. Billups, and A. Morgan. Algorithm 652: Hompack: A suite of codes for globally convergent homotopy algorithms. *ACM Transactions on Mathematical Software (TOMS)*, 13(3):281–310, 1987.
- [47] J. Xu. Iterative methods by space decomposition and subspace correction. *SIAM review*, 34(4):581–613, 1992.
- [48] J. Xu, L. Chen, and R. Nochetto. Optimal multilevel methods for h (grad), h (curl), and h (div) systems on graded and unstructured grids. *Multiscale, nonlinear and adaptive approximation*, 1(1):599–659, 2009.
- [49] Z. Zeng. Algorithm 835: Multroot—a matlab package for computing polynomial roots and multiplicities. *ACM Transactions on Mathematical Software (TOMS)*, 30(2):218–236, 2004.
- [50] Z. Zeng. Computing multiple roots of inexact polynomials. *Mathematics of Computation*, 74(250):869–903, 2005.